To See, Not to See, or to See Poorly: Perceptual Quality and Guess Rate as a Function of Electroencephalography (EEG) Brain Activity in an Orientation Perception Task

Sarah S. Sheldon[1] and Kyle E. Mathewson[1-2]

[1]University of Alberta, Department of Psychology, Faculty of Science

[2]University of Alberta, Neuroscience and Mental Health Institute, Faculty of Medicine and Dentistry

Author Note

Sarah S. Sheldon https://orcid.org/0000-0002-4026-8939

Kyle E. Mathewson https://orcid.org/0000-0003-4856-3980

This research was supported by start-up funds from the Faculty of Science and an NSERC Discovery grant (#RES0024267) awarded to Kyle Elliot Mathewson. The authors would like you thank Erron Jacob Meneses, Jenny Le, and David Lam for assistance in data collection, and Daniel Robles and Jonathan Kuziek for analysis feedback.

Correspondence concerning this article should be addressed to Sarah S. Sheldon, Department of Psychology, University of Alberta, Edmonton, Alberta, T6G 2R3, Canada. Email: ssheldon@ualberta.ca

Abstract

Brain oscillations are known to modulate detection of visual stimuli, but it is unclear if this is due to increased guess rate or decreased precision of the mental representation. Here we estimated quality and guess rate as a function of electroencephalography (EEG) brain activity using an orientation perception task. Errors on each trial were quantified as the difference between the target orientation and the orientation reported by participants with a response stimulus. Response errors were fitted to standard mixed model by Zhang and Luck (2008) to quantify how participants' guess rate and standard deviation parameters varied as a function of brain activity. Twenty-four participants were included in the analysis.

Within subjects, the power and phase of delta and theta post-target oscillatory activity were found to vary along with performance on the orientation perception task in that greater power and phase coherence in the 2-5 Hz band range was measured in trials with more accurate responses. In addition, the phase of delta and theta correlated with the degree of response error while oscillatory power did not have a relationship with trial-by-trial response errors. Analysis of task-related alpha activity yielded no significant results implying that alpha oscillations do not play an important role in orientation perception at single trial level. Across participants, only the standard deviation parameter correlated with oscillatory power in the high alpha and low beta frequency ranges. These results indicate that post-target power is associated with the precision of mental representations rather than the guess rate, both across trials within subjects and across subjects.

Keywords: EEG, time-frequency analysis, orientation perception, standard mixed model, visual perception

To See, Not to See, or to See Poorly: Perceptual Quality and Guess Rate as a Function of Electroencephalography (EEG) Brain Activity in an Orientation Perception Task

Variations in neural activity give rise to observed variations in our visual perception. (Chaumon & Busch, 2014; Mathewson et al., 2011; Samaha et al., 2020). While there has been a plethora of research into the brain activity that drives this process, there remains noticeable gaps in our understanding of how these processes work. One of the reasons for this might be because investigators have left basic questions about the underlying neural mechanisms unanswered. Specifically, does perception have an all-or-none principle where a certain threshold must be met before a perceptual representation can form; or, does a perceptual representation always form but the quality depends on the state of the neural activity? It seems unlikely researchers can form a deep understanding of these perceptual processes without first determining what kind of process we are looking at.

Traditionally, visual perception has been studied with two-alternative forced-choice (2-AFC) tasks or similar discrete response paradigms. In these types of paradigms, participants are required to select one out of two or more possible responses. Sometimes they are asked to choose the correct stimulus out of an array of different stimuli or to simply report whether they detected a visual stimulus. Although informative, these paradigms might miss certain aspects of visual perception that cannot be measured with only two or three discrete categories. Continuous behavior allows for more interpretable statistical measures since many of the common descriptive and inferential statistics rely on the assumption of continuous measures. Furthermore, while there are numerous inferential models based on the discrete response paradigms, it is unclear whether these models are the best approach for investigating the neural mechanisms underlying the perceptual responses they were designed for. In particular, the question about

what type of process underlies the formation of perceptual representations cannot be addressed without a way to independently measure perceptual detection and perceptual quality.

To answer the question about the nature of perceptual processes, we need a task that can measure visual perception on a continuous scale and a model that can quantify perceptual responses in a way that will inform our question. With this goal in mind, we developed the orientation perception task. The orientation perception task is an adaptation of Bae and Luck's (2018) orientation memory task. The researchers originally used their task to investigate how well information held in working memory can be decoded from brain activity. What makes the task useful for the current study is that it allows participants to give a continuous response when asked to report the orientation of the target. Performance can then be quantified as the angular difference between the orientation of the target and the orientation reported by the participants, referred to as response errors. This continuous measure of response errors can utilize a standard mixed model introduced by Zhang and Luck (2008) to quantify parameters of interest such as guess rate and precision of the perceptual representation. We here extend this method in order to look for evidence of either all-or-none or graded perceptual mechanisms, and determine whether these processes are individually related to electrical brain activity during the task.

To address the question about the type of process underlying visual perception, we combined our adapted version of the visual orientation task with the standard mixed model and electroencephalography (EEG). Because there are several novel parts in the current study, the purpose was two-fold. First, we asked whether the standard mixed model could be extended to a visual perception task? Second, we tested the hypothesis that there was a relationship between EEG oscillatory activity, specifically in the alpha frequency band, and the standard mixed model parameters (guess rate and standard deviation). To address these questions, we modified an

orientation memory task from Bae and Luck's (2018) so that it probed participants' perception of the target's orientation rather than their ability to remember it. We then recorded EEG activity as participants performed the adapted task so we can see how brain activity varies with their perceptual performance.

Materials and Methods

Participants

Twenty-eight participants from the University of Alberta community participated in the study (age range = 17-35 years). Two participants were not included in the analysis due to excessive movement artifacts (more than 25% of trials rejected due to artifacts). Another two participants were excluded from the analysis due to having extreme outlying performance on the task (see Behavioral Analysis in the Results section for more details). Participants were all right-handed and had normal or corrected normal vision and no history of neurological problems. All participants gave informed written consent, were either compensated at a rate of $10/hr or given research credit for their time. The study adhered to the tenets of the Declaration of Helsinki and was approved by the Internal Ethics Board at the University of Alberta.

Orientation Perception Task

Participants were seated 57 cm away from a 1920 x 1080 pixel^2 ViewPixx/EEG LCD monitor (VPixx Technologies, Quebec, Canada) with a refresh rate of 120 Hz, simulating a CRT display with LED backlight rastering. The rastering, along with 8-bit digital TTL output triggers yoked to the onset and value of the top left pixel, allowed for submillisecond accuracy in pixel illumination times, which were confirmed with a photocell prior to the experiment. Stimuli were presented using a Windows 7 PC running MATLAB R2012b with the Psychophysics toolbox (Version 3; Brainard, 1997; Pelli, 1997). The code running the task was a modified version of the

ColorWorkingMemoryExperiment.m code from MemToolbox (Suchow et al., 2013; memtoolbox.org). The modified version of color working memory experiment can be found here: https://github.com/APPLabUofA/OrientTask_paper/tree/master/OrientationTask. Video output was sent to the ViewPixx/EEG with an Asus Striker GTX760 (Fremont, CA) graphics processing unit.

Each trial began with a white fixation dot presented at the center of the monitor for 742, 783, 825, or 867 ms (target stimulus onset asynchrony; tSOA) after which the target appeared for 8.33 ms (one monitor refresh). The target was in the shape of a needle and was pointing toward one of 24 predefined evenly spaced directions so that all the orientations covered 360 degrees. The direction of the target was randomly selected on each trial. Of all the trials, 20% were randomly chosen not to have a target. All aspects of the target-present and target-absent trials were identical except that for the target-absent condition a blank interval replaced target presentation. A backward mask lasting for 8.33 ms with a constant 41.7 ms target-mask SOA (mSOA) appeared centrally. The mask was created by overlaying the target orientated in all 24 directions which created a star shape seen in Figure 1A. Following the mask offset, a 500 ms blank interval period occurred.

After the blank interval, a response screen appeared with the needle in the center of the screen. Using the computer mouse, participants were asked to rotate the needle so that it was pointed in the same direction as the previous target. If participants detected a target but could not remember its orientation, they were asked to guess the orientation of the target. Participants could provide their response at their own pace. No feedback was given to participants. The next trial began immediately after a needle's orientation was selected. See Figure 1A for a summary of the task sequence and the stimulus dimensions.

Participants completed seven blocks consisting of 48 trials each, along with 20 practice trials at the beginning of the experiment. Participants could rest at their own pace every 48 trials. Extensive written and verbal instructions were presented to participants prior to the practice trials. Instructions thoroughly explained and demonstrated each component that would compose a single trial.

Before the orientation perception task, participants performed a staircased target detection task that had the same parameters as the orientation perception task except that participants only reported whether they saw the target or not using the keyboard. The target color was a gray determined by a scalar value passed to the functions in Psychtoolbox. In the staircased target detection task, the target color value could range from the background color (making it not visible; corresponding value of 256) to black (making it the most visible; corresponding value of 0). This target gray value was adjusted throughout the task based on a 1-up/2-down staircasing procedure targeting a 0.6 target detection rate for each individual (García-Pérez, 1998; Kingdom & Prins, 2016). The staircased task consisted of three blocks of 32 trials. The target gray value was determined for each participant by taking the average target gray value across the last two blocks of trials. These final average values ranged from 70 to 112 and were used as the target gray value in the orientation perception task.

The MATLAB code for the a staircased target detection task and the orientation perception task are available at https://osf.io/cw7ux/ and https://github.com/APPLabUofA/OrientTask_paper.

EEG Recording

During the experiment, EEG data was recorded from each participant with a Brain-Amp 32-channel amplifier (BrainVision) using gelled low-impedance electrodes (actiCAP passive

electrodes kept below 5 kΩ). Inter-electrode impedances were measured at the start of each experiment. All electrodes were arranged in the same 10-20 positions (Fp2, Fp1, F4, F3, F8, F7, FC2, FC1, FC6, FC5, C4, C3, CP2, CP1, CP6 CP5, P4, P3 P6, P5, P8, P7, PO4, PO3, O2, O1, Fz, FCz, Cz, Pz, and Oz). In addition to the 31 EEG sensors, a ground electrode was used, positioned at AFz. Two reference electrodes and the vertical and horizontal bipolar EOG were recorded from passive Ag/AgCl easycap disk electrodes affixed on the mastoids, above and below the left eye, and 1 cm lateral from the outer canthus of each eye. The bipolar channels were recorded using the AUX ports of the Brain-Amp amplifier. SuperVisc electrolyte gel and mild abrasion with a blunted syringe tip were used to lower impedances. Gel was applied and inter-electrode impedances were lowered to less than 5 kΩ for all electrode sites. EEG data was recorded online referenced to an electrode attached to the left mastoid. Offline, the data were re-referenced to the arithmetically derived average of the left and right mastoid electrodes.

Data were digitized at 1000 Hz with a resolution of 24 bits. Data were filtered with an online bandpass with cutoffs of 0.1 Hz and 250 Hz. The experiment was run in a dimly lit, sound and radio frequency-attenuated chamber from Electromedical Instruments, with copper mesh covering the window. The only electrical devices in the chamber were an amplifier, speakers, keyboard, mouse, and monitor. The monitor ran on DC power from outside the chamber, the keyboard and mouse were plugged into USB outside the chamber, and the speakers and amplifier were both powered from outside the chamber, and nothing was plugged into the internal power outlets. Any devices transmitting or receiving radio waves (e.g., cell phones) were removed from the chamber for the duration of the experiment.

EEG Preprocessing

All analyses were completed using Matlab R2018b with the EEGLAB 13.6.5b (Delorme & Makeig, 2004) and CircStat (Berens, 2009) toolboxes, as well as custom scripts. After the data had been re-referenced offline, the bandpass FIR filter from EEGLAB was applied with lower and upper cut-offs of 0.1 Hz and 50 Hz. Data was segmented into 3000 ms epochs aligned to target onset (-1500 ms pre-target onset to 1500 ms post-target onset). The average voltage in the 200 ms baseline prior to the target was subtracted on each trial for every electrode, and trials with absolute voltage fluctuations on any channel greater than 1000 μV were discarded. Eye movements were then corrected with a regression-based procedure developed by Gratton, Coles, and Donchin (1983). After a second baseline subtraction with 200 ms pre-target, trials with remaining absolute voltage fluctuations on any channel greater than 500 μV were removed from further analysis. Data was then subjected to visual inspection and manual rejection of trials contaminated by artifacts. On average, 3% of trials were rejected during visual inspection. Other than the two participants mentioned earlier, none of the remaining participants had more than 20% of trials rejected in this manner.

Data Analyses

Data analysis was performed using MATLAB R2018b (The MathWorks Inc, Natick, MA, USA) and EEGLAB 13.6.5b (Delorme & Makeig, 2004). All statistical analyses were conducted using MATLAB R2018b. Red-white-blue colormaps were created using the redblue.m function by Auton (2009) found here: https://www.mathworks.com/matlabcentral/fileexchange/25536-red-blue-colormap. The MATLAB code for data analysis is available at the GitHub repository https://github.com/APPLabUofA/OrientTask_paper and the raw data files are available at https://osf.io/cw7ux/.

Behavioral Data

Response errors on each trial were calculated by subtracting the orientation of the response stimulus, as reported by the participant, from the orientation of the target stimulus (see Figure 1B). The standard mixed model proposed by Zhang and Luck (2008) was fit to each participant's response errors using the maximum likelihood estimation routine in the MemToolbox (Suchow et al., 2013). According to the standard mixture model, response deviations from the actual target orientation reflect a mixture of trials where the target's orientation was detected and trials where participants did not detect the target so guessed randomly. Therefore, the distribution of response errors consists of a mixture of a von Mises distribution (representing the trials where the target's orientation was detected) and a uniform distribution (random guesses (g)). Parameter sigma (σ) is the standard deviation of the von Mises distribution, which represents the width of the response error distribution of trials that the target's orientation was detected. Parameter g is the height of the uniform distribution representing the guessing probability. A third parameter, mu (μ), which is the mean of the von Mises distribution and represents systematic bias of the response error distribution was included in the standard mixture model of two participants because the Bayesian information criterion (BIC), calculated with the model comparison functions provided by MemToolbox (Suchow et al., 2013), indicated that the three-parameter standard mixture model provided better fits for those two participants (see Table 1). Although the three-parameter model was used for all analysis of those two participants, the systematic bias was much smaller than the spacing between adjacent target orientations (spacing was 15° whereas the two participants' μ was -4.2° and 2.7°) indicating that those two participants had a slight clockwise and counterclockwise bias, respectively. The two-parameter standard mixture model was used for all analysis of the remaining 22 participants

because it provided a better fit according to the BIC.

Time-Frequency Analyses

To calculate the phase angle and power for each trial, we used Morlet wavelet transform of single trials using the newtimef() function of EEGLAB. A Morlet wavelet is a tapered sinusoid, constructed by modulating a sine wave with a Gaussian envelope. Wavelet transformation was created with 1.027 Hz linear steps and cycles starting from 2 cycles at 2 Hz to 12 cycles at 40 Hz. The output of this function was a matrix of complex values. The abs() function from MATLAB was used to get the instantaneous amplitude and the instantaneous phase angle of each trial was calculated using the angle() function from MATLAB.

Oscillatory power data was converted to *Z* scores by applying a single-trial normalization procedure to the data from each participant at each electrode and frequency separately. This was done because it helps disentangle background from task-related dynamics, allows for comparison across different frequency bands and electrodes, and facilitates group-level analysis (Cohen, 2014). Each trial's entire epoch was used for the baseline during normalization because it has been shown to be robust to the effects of noisy trials and is still conducive for analysis of pre- and post-target activity (Grandchamp & Delorme, 2011). The downside to using the entire epoch for the baseline normalization is that sustained changes throughout the trial period become difficult to detect (Cohen, 2014). Ultimately, we considered this an acceptable trade-off for being able to analyze oscillatory power and behavioral measures across participants without having to make assumptions about frequency bands and time-windows such as would be required for "binning" analysis used in previous studies (Barne et al., 2020; Iemi et al., 2017; Limbach & Corballis, 2016; Samaha et al., 2017).

Accurate vs Guess Trials

To test for significant differences in brain activity on trials where participants had small response errors compared to large response errors, we separated each participant's trials based on the sigma value from the fits of their individual response errors to the standard mixed model. This was done by defining each participant's trials with response errors between -0.75σ and +0.75σ as "accurate," and trials with response errors less than -1.5σ and greater than +1.5σ as "guesses" (Figure 2A). The logic is that trials). Trials where the participant clearly perceives the target are likely trials with a response error less than the participant's overall response standard deviation, and trials the participant has little to no perception of the target are likely trials with a response error greater than just the participant's response standard deviation. It should be noted that there are various reasons for participants to be accurate when they are guessing or have a large response error when they accurately perceived the target. However, such events are thought to be rare enough, or at least not systematic, that they will not unduly affect the overall distribution.

The main reason we separated trials into "accurate" or "guess" was to see if the standard mixed model parameters could be used to categorize trials in a meaningful way. Though this method resulted in excluding some trials, namely ones that fell between the cutoffs for accurate and guess, the outcome provided insight into how brain activity differs between different levels of objective perceptual performance.

ERP Analyses. To remove the activity elicited by the mask without removing activity resulting from the interaction of mask and target, the catch trials (mask-only) average was subtracted from the orientation detection trials (target-plus-mask) average. ERP data was submitted to a repeated measures, two-tailed permutation test based on the *tmax* statistic (Blair & Karniski, 1993) using the mxt_perm1() function from the Mass Univariate ERP Toolbox (Groppe et al., 2011). The time windows of interest were the P1 (80-140 ms), N1 (140-200 ms), P2 (200-255 ms), N2 (255-360 ms), and P3 (360-500 ms) components. The ERP component time windows were selected based on previous literature (Koivisto & Revonsuo, 2003, 2010). All 31 brain electrodes were included in the test. 100,000 random within-participant permutations were used to estimate the distribution of the null hypothesis and the family-wise alpha (α) was set to 0.05. Based on this estimate, critical *t*-scores of +/-3.68 (df = 23) were derived. Any t-scores that exceeded the critical *t*-score were considered statistically significant.

Oscillatory Power Analysis. To analyze differences in EEG band power between guess and accurate trials, nonparametric permutation testing with a pixel-based multiple-comparison correction procedure (Cohen, 2014) was used to analyze differences in EEG band power between guess and accurate trials. The pixel-based multiple-comparison correction method involves creating one distribution of the largest positive pixel value and another distribution of the largest negative pixel value from each iteration of the permutation testing. After all iterations, the statistical threshold is defined as the value corresponding to the 2.5^{th} percentile of the smallest values and the value corresponding to the 97.5^{th} percentile of the largest values which are the thresholds corresponding to an α of 0.05. Any pixel that has a value exceeding the upper or lower value is considered significant. The pixel-based method corrects for multiple comparisons by creating two distributions based on map-level information instead of pixel-level information. In

other words, this method results in two distributions of the most extreme null-hypothesis test statistical values across all pixels rather than calculating null-hypothesis distributions for each pixel (see Cohen (2014) for further details about pixel-based multiple-comparison correction method). All analysis using nonparametric permutation testing with pixel-based multiple-comparison correction performed 10,000 iterations per test. To obtain more stable estimates from permutation testing, we ran a “meta-permutation test” by repeating the pixel-level permutation procedure 10 times and then averaging the results (Cohen, 2014). It needs to be pointed out that a “significant effect” determined by pixel-based permutation testing should not be considered a precise estimate in the temporal and frequency domains. Although pixel-based permutation testing is more stringent than cluster-based permutation tests (Cohen, 2014), caution should still be used when interpreting “significant” differences, especially if the temporal and frequency range of each pixel is relatively small.

Oscillatory Phase Analysis. To determine whether the mean phase values significantly differ between accurate and guess trials, we used the circular Watson–Williams (W-W) test which was calculated using the PhaseOpposition.m function by VanRullen (2016). We chose the parametric circular W-W test because it has shown to be equivalent to the non-parametric phase opposition sum (POS) measures under most conditions, and performed better in situations where either the relative trial number or the ERP amplitude differed between the two trial groups (VanRullen, 2016). The statistical significance of the W-W test across participants was determined by combining the individual-level *p*-value time-frequency map at each electrode across participants using Stouffer's method (Stouffer et al., 1949; VanRullen, 2016), which transforms individual *p*-values into *z*-scores, combines them across participants, and converts the resulting *z*-score to a combined probability. *P*-values were then corrected for multiple

comparisons across time points and frequencies at each electrode using the false discovery rate (FDR) procedure described in Benjamini and Yekutieli (2001). Effects that satisfied a 5% FDR criterion were considered significant.

Single-Trial EEG Activity and Response Errors

To test the correlation between time-frequency power and degree of response error, Spearman's rho (r_s) correlation coefficients were calculated using a nonparametric permutation testing approach with the pixel-based multiple-comparison correction procedure described above. The null-hypothesis distribution was created by shuffling power values and response errors on each trial with respect to each other. This provided a data-driven test of the null hypothesis that there is no consistent relationship between degree of response error and EEG power.

To look at whether task performance is related to oscillatory phase, and if yes, at what frequency, we used the weighted inter-trial phase clustering (wITPC) (Cohen, 2014; Cohen & Voytek, 2013). The logic behind the inter-trial phase coherence (ITPC) is that a systematic relation between EEG phase and behavioral outcome should result in a higher-than-chance ITPC in each of the trial subgroups. However, if the phase of the EEG signal is randomized and unpredictable, the distribution of phases at a given time period should follow a uniform distribution over all trials. The problem with ITPC is that it assumes EEG phase is relevant to experimental measures only when phase values are similar across trials (van Diepen & Mazaheri, 2018). Unlike ITPC, wITPC is sensitive to modulations of phase values even if those phases are randomly distributed across trials as would be expected if response errors (which differs from trial to trial) were modulated by oscillatory phase (Cohen, 2014; Cohen & Voytek, 2013).

The wITPC was computed for each participant as the resultant vector length, or ITPC, of phase angles across trials once the length of each vector has been weighted by a variable of

interest (in this case, each trial's phase vector is weighted by the degree of response error on that trial; see Figure 4A for example of computation) (Cohen, 2014; Cohen & Voytek, 2013). For statistical testing, a null-hypothesis distribution was created by shuffling the phase values relative to trial response error 10,000 times (see Figure 4A middle and bottom left). The wITPCz was calculated as the wITPC standardized relative to the null-hypothesis distribution, providing a *z*-value corresponding to the probability of finding the observed response error–phase modulation by chance, given the measured data. To evaluate statistical significance of the wITPCz across participants, we combined the individual-level *p*-value, calculated from the *z*-values, time-frequency map at each electrode across participants using Stouffer's method (Stouffer et al., 1949; VanRullen, 2016). *P*-values were then corrected for multiple comparisons across time points and frequencies at each electrode using the false discovery rate (FDR) procedure described in Benjamini and Yekutieli (2001). Effects that satisfied a 5% FDR criterion were considered significant.

We chose to use the phase opposition measure and the wITPCz even though they are both quantifying oscillatory phase because they provide different but complementary information about the effects of phase. The phase opposition measure provides insight into whether there is an overall consistent difference in the response-related (*i.e.*, "accurate" and "guess" response) mean oscillation phase values. On the other hand, the weighted single-trial phase modulation metric (*i.e.*, wITPCz) provides information about process-specific modulations of phase values even when the phase distribution across trials is not consistent (Cohen, 2014; Cohen & Cavanagh, 2011). In other words, phase values do not need to be consistent over trials, they only need to be consistently related to response errors (Cohen & Cavanagh, 2011). This is an important

distinction when trying to determine how much of the phase modulation is an artifact of the stimulus-evoked activity and how much is related to the difference in task performance.

Relationship Between Oscillatory Power and Standard Mixed Model Parameters

For testing the relationship between time-frequency power and each participant's standard deviation and guess rate parameter, Spearman's rho (r_s) correlation coefficients were calculated using a nonparametric permutation testing approach with the pixel-based multiple-comparison correction procedure described above. The null hypothesis correlation coefficients were produced by randomly reassigning participant's estimated parameter values from the standard mixed model (guess rate or standard deviation) to other participants then recomputing r_s.

Results

Accurate vs Guess Trials

Two participants were excluded before further analysis because one had a guess rate more than three *IQR*s from the median and the other had a guess rate of 3.9e-15 indicating that the staircasing procedure did not work properly for this individual. These participants were not included in further analysis. Figure 2B shows the fit of the standard mixed model (or standard mixed model with a bias parameter for the participants mentioned in the Methods section) to each participant's response errors as well as the average fit of response errors across participants. The remaining 24 participants had a mean guess rate of 0.19 (*SD* = 0.18) and mean standard deviation (σ) parameter of 11.1 (*SD* = 2.5). The boxplots in Figure 2C summarizes the distributions.

ERP Analysis

The ERPs from accurate and guess trials (Figure 3A) showed no statistical difference for the first 200 ms following target onset across all electrodes. A divergence in the waveforms can

be seen in the P2 (200-300 ms) component for the frontal, central, and centroparietal electrodes (Figure 3B left) in that the voltage of the guess trial ERPs was much attenuated compared to the accurate trial ERPs. On the other hand, the voltage of the N2 (255-360 ms) component was more negative in the guess trials than accurate trials (Figure 3A) and this difference was only significant in the right frontocentral, central, centroparietal and parietal electrodes (Figure 3B middle). Finally, the P3 (360-500 ms) component from the guess trials had a similar attenuation as was seen in the P2 component (Figure 3A), but the distribution was more posterior with significant effects seen in the right central, centroparietal and parietal electrodes as well as bilateral parietooccipital and occipital electrodes (Figure 3B right).

Oscillatory Power Analysis

Pixel-based permutation test indicated significant differences between accurate and guess trials within the lower part of the theta band and the delta band (2-4 Hz) which was observed to start around 300 ms post-target onset in P8 and 350 ms post-target onset in P7 and had a duration of around 75 ms (Figure 3C). Fp2 (not shown) showed a significant difference between accurate and guess trials at around 325 ms to 385 ms post-target in the delta band (2-3 Hz) while P5 (not shown) had a significant difference in the delta band (2-3 Hz) starting at around 450 ms post-target with a duration of about 130 ms (extending to shortly after response screen onset). Finally, the P3 electrode showed a brief significant difference in power at 6 Hz at about 330 ms post-target (Figure 3C).

Overall, there was a trend for increased theta power in accurate trials compared to guess trials, especially in left frontal and right parietal areas, though this difference was not significant except for what is mentioned above. This lack of significance might be due to too much variability in when theta power changed during the trial. It is also possible that theta reflects a

perceptual process that could occur in both accurate and guess trials, though more often or to a greater degree in one type of trial compared to the other.

Oscillatory Phase Analysis

Similar to the oscillatory power results, significant differences in mean phase between accurate and guess trials were found in the delta and theta frequency ranges following target onset (Figure 3D). Central and bilateral frontal, frontocentral, and central electrodes show significant phase differences in theta starting between 150-200 ms and terminating before 350 ms post-target (not shown). The duration of this effect varies so that the more central electrodes tended to have longer durations than those placed more laterally on the head. This effect was more prevalent in the right hemisphere in the early period.

The most lateral parietal and centroparietal electrodes on the left side of the head show significant phase differences in delta after the response screen onset. On the other hand, Pz, P3 (Figure 3D), P4, and PO3 electrodes had no significant effects in phase while P6 and P8 had brief periods of significant phase differences starting a little after 300 ms until 500 ms post-target in the delta frequency range. P7 showed a similar significant difference in mean phase at 2 Hz starting around 225 ms and continuing until more than 200 ms after the response screen had been presented (about 770 ms post-target; Figure 3D). The occipital electrodes had significant phase effects primarily in the low theta and delta range (3-5 Hz) starting a little after 100 ms on the left (not shown) and 150 ms on the right but were brief time periods until 200 ms post-target which then had significant differences lasting for about 200 ms (Figure 3D). PO4 electrode showed a similar difference, but the effect was less continuous and had larger *p*-values (*i.e.*, smaller phase difference between accurate and guess trials) than the occipital electrodes; however, PO4 also had significant differences in delta between 400 and 500 ms (Figure 3D).

It should be noted that the time window of significant phase opposition overlaps with the significant differences in ERP amplitudes. ERP amplitudes have been shown to have a “masking” effect on phase opposition measures resulting in a decrease in their statistical power (VanRullen, 2016) while at the same time the stimulus-evoked activity results in temporal distortion of oscillatory activity towards earlier latencies (Brüers & VanRullen, 2017). While the circular W-W test is relatively robust against the detrimental effect of ERPs, it does not negate their influence entirely (VanRullen, 2016). Therefore, it is important to be aware that the significant effects of phase are affected by the stimulus evoked activity and the different ERP amplitudes between accurate and guess trials.

Single-Trial EEG Activity and Response Errors

To see whether response errors were related to trial-by-trial changes in pre-target alpha power, the Spearman’s rho correlations were calculated between oscillatory power and degree of response error on each trial. Our results did not allow us to reject the null hypothesis. Follow-up analysis on the entire time-frequency space also yielded no significant results. This is in line with the lack of significant correlations between oscillatory power and guess rate (not shown).

To examine the relationship between response errors and the distribution of phase values, we used the wITPCz. As can be seen in Figure 4B (bottom row), phase was primarily modulated by degree of response errors in the delta frequency range in the posterior electrodes starting at around 200 ms post-target and lasting until response screen onset. PO3 was similar except the effect started at around 250 ms (not shown), but PO4 showed an effect starting at 350 ms and lasting until almost 100 ms after the response screen onset (Figure 4B, bottom row). Parietal electrodes show a significant effect in the low frequency bands starting at around 200 ms until about 800 ms post-target (Figure 4B, top and bottom rows). Centroparietal and central electrodes

had a significant relationship between delta phase and response errors at around 300-400 ms post-target and lasted until after response screen onset (not shown). All frontocentral electrodes had response errors significantly related to delta phase starting between 200 ms and 300 ms post-target and lasting until shortly after response screen onset (not shown). Out of all the frontal electrodes, only Fz and F3 had a significant delta and theta phase relationship to response errors (not shown).

Relationship Between Oscillatory Power and Standard Mixed Model Parameters

Using pixel-based multiple comparison correction procedure and Spearman's rho (r_s), power at each pixel across time-frequency space was correlated with participants' parameter values calculated from their response errors being fit to the standard mixed model. Results indicate the oscillatory power and standard deviation (σ) parameter were significantly positively correlated in right parietal, parietooccipital, occipital and central occipital electrodes (Figure 5). The significant correlations were mostly in the alpha and low beta frequency ranges and occurred between a time window starting at around 150 ms and ending at 440 ms post-target onset. The exceptions were F3 and F4 (not shown) that showed significant positive correlations between with the standard deviation parameter and power in the 3 Hz range during the onset of the response screen for around 50 ms. The same analysis was done on oscillatory power and guess rate which yielded no significant correlations though there was a trend towards a negative correlation between guess rate and high alpha/low beta oscillatory power (not shown), especially in more frontal electrodes.

Discussion

There were two goals for the present study. First, we asked what might the relationship be between the parameters of the standard mixed model and EEG activity? We were successful in

this first goal: application of the standard mixed model to a visual perception task and relating that performance measure and model parameters to EEG brain activity recorded during the task. The second goal was to try to answer the question of how brain activity modulates perceptual representation. Specifically, we wanted to see whether perception has an all-or-none principle where a certain threshold must be met before a perceptual representation can form; or, if a perceptual representation always forms but the quality depends on the state of the neural activity. The results from the current study strongly point towards visual perception operating by the latter principle rather than the former.

Accurate vs Guess Trials: ERP Activity

Significant differences in ERP waveforms of the accurate and guess trials started at around 200 ms post-target onset in the anterior locations on the head (Figure 3B) which corresponds to the P2 component (Di Russo et al., 2019; Key et al., 2005; Potts & Tucker, 2001). The greater amplitude of the P2 for accurate guess trails fits with the P2 being related to the salience of stimuli (Potts & Tucker, 2001) or stimulus recognition (Harel et al., 2016). We also observed a more negative N2 for guess trials, that seems to go against current literature which suggests that the onset of visual consciousness can be marked by a greater negativity in the N2 time range due to an overlapping posterior negative component called the visual awareness negativity (VAN) (Förster et al., 2020; Koivisto & Revonsuo, 2003, 2010). However, the separation of trials based on response performance rather than awareness (according to Koivisto and Revonsuo (2010), the VAN can only be reliably detected by comparing aware and unaware conditions), would explain why we would not expect greater negativity in the N2 time range for accurate ERPs compared to guess ERPs. Furthermore, the distribution of the observed N2 component (mostly right central electrodes) does not match the typical posterior VAN

distribution (Förster et al., 2020). In fact, the N2 distribution points towards the presence of the much larger P3 component. The most likely explanation is that the attenuated guess trial ERPs (compared to accurate trials) results in a smaller or later positive voltage from the much larger P3 overlapping the negative deflection at the N2 time period (Förster et al., 2020; Koivisto & Revonsuo, 2010) so that the N2 appears more negative in guess trials when it is actually due to the P3 being smaller. The voltage increase of accurate compared to guess ERPs during the P3 time window follow previous findings on attention and visual perception (Key et al., 2005; Salti et al., 2012). In the current study the P3 is likely related to processes such as stimulus classification and saliency evaluation (Doradzińska et al., 2020; Förster et al., 2020; Helfrich & Knight, 2019; Salti et al., 2012) and that these processes are overwhelmingly more relevant to accurate orientation perception than processes for conscious perception as reflected by the relatively smaller N2 ERP. Furthermore, the difference in ERPs between accurate trials and guess trials during the N2 time period (see middle topographic plot of Figure 3B) indicates that the processes reflected by the N2 likely occur in both types of trials though to differing degrees. Instead, it appears that the main difference between accurate and guess trials is the extent that the target can be classified or evaluated by the brain regardless of consciously perceiving the target.

Accurate vs Guess Trials: EEG Oscillatory Activity

We had originally hypothesized alpha activity, especially prior to target onset, mediating task performance. However, the results did not support this hypothesis. As a visual perception task, this might be surprising. There has been a recent accumulation of evidence suggesting pre-target alpha power modulates visual detection performance by changing baseline neural excitability (Iemi et al., 2019; Samaha et al., 2017, 2020). This might be attributed to using both pre- and post-target activity in the pixel-based multiple correction procedure. Relative to post-

target activity, pre-stimulus power would be very small since the only thing for participants to do was fixate on a white circle. As a result, differences in pre-target activity might not exceed significance thresholds when those thresholds were based on the background spectra of the combined pre- and post-target activity. However, we tested this possibility by analyzing power in the alpha frequency during just the pre-target time period and found no significant differences between accurate and guess trials (data not shown). Therefore, it is unlikely that a lack of significant difference in pre-target alpha is due to an exceedingly high statistical threshold set by the post-target activity.

The most likely reason for not finding a pre-target effect of alpha activity is that there was no information for the participant to use before a target was presented, so there would be no attention-related changes or task-based preparation prior to the target. The absence of significant effects in post-target alpha oscillations suggests that alpha activity is not related to the processes responsible for differences between accurate and guess trials. The fact that post-target alpha activity was also unrelated to response errors on a trial-by-trial basis suggests that alpha activity is not related to perception of a target's orientation. This is consistent with Bae and Luck (2018) who found that alpha activity did not encode a target's orientation when the target's spatial location was controlled for. An absence of a relationship between alpha power and performance measures has been noted in other studies though they were not able to rule out changes in detection bias which can be ruled out in the current study since guess rate was not related to alpha activity (Benwell et al., 2017; Keitel et al., 2018). However, awareness bias might be a possibility assuming orientation perception can proceed in the absence of conscious awareness which seems likely based on previous research (Benwell et al., 2017; Doradzińska et al., 2020; Koenig & Ro, 2019). In sum, it is likely that alpha oscillations are more related to a global

process that is not dependent on conscious awareness and would not change across trials such as feature-independent stimulus processing.

The most significant differences between accurate and guess trials were in the delta and low theta (2-4 Hz) frequency ranges, particularly in the parietal and parietooccipital electrodes during the latter half of the post-stimulus epoch (Karakaş, 2020). A significant increase of delta and low theta power in accurate compared to guess trials could be seen at around 300 ms though their differences in mean phase, especially for theta, started earlier (200 ms post-target). Although there was a trend in our data for increased theta power in accurate trials compared to guess trials, this difference was not reliable.

The significant differences in theta and delta seem to correspond to changes in the N2 and P3 ERP components observed in the time domain. Many studies have shown that delta and theta are the primary contributors to the formation of the N2 and P3 (Harmony, 2013; Harper et al., 2014; Karakaş et al., 2000). It has been proposed that delta contributes continuous positivity throughout the ERP response while theta activity corresponds to the polarity change as the negative deflection during the N2 shifts to the positive deflection during the P3 (Harper et al., 2014). This fits with the observed oscillatory activity of accurate and guess trials (Figure 3C and 3D). Furthermore, the interplay between theta and delta oscillations would explain the indistinct N2 but large P3 waveforms (Karakaş et al., 2000).

The increase in theta power during accurate trials relative to guess trials has the earliest onset in left frontal and right parietal electrodes. Prolonged theta in right posterior electrodes is accompanied by significant differences in mean (low) theta phase between accurate and guess trials. Theta has been interpreted as being correlated with selective attentional processing (Başar et al., 2001; Karakaş, 2020; Karakaş et al., 2000) and an increase in theta synchronization and

power has been associated with successful memory encoding (Klimesch, 1999) and right hemispheric theta is greater than left when encoding visuospatial information (Sauseng et al., 2004). Although the task in this study was not a memory task, encoding information is still a viable way of looking at how the brain transforms the visual sensory information into perceptual representations. In fact, theta has been shown to be sensitive to target and non-target stimuli regardless of memory load (Palomäki et al., 2012). Therefore, it is probable that theta activity might be related to the "encoding" of the target's orientation or just the detectability of target itself. Both functions could occur in accurate and guess trials, though more often or to a greater degree in accurate trials compared to guess trials. This would explain why theta oscillations showed a for trend increased power in accurate trials compared to guess trials though this difference was usually not significant.

In contrast to theta, delta showed a more spatially diffuse increase in power in accurate vs guess trials with maxima over the lateral parietal areas. Delta phase differed significantly between accurate and guess trials over the occipital and lateral parietal areas with the most robust phase differences at around 350 ms post-target. Several experiments that showed increases in delta activity during the performance of different mental tasks and conflict-monitoring paradigms have led investigators to associate delta with modulation of networks that should be inactive to accomplish the task (Harmony, 2013; Rawls et al., 2020). Investigators have also noted a close association between delta oscillations and the P3 ERP waveform (Harper et al., 2014; Rawls et al., 2020; Schürmann et al., 1995, 2001). If the P3 reflects post-perceptual processes, then it is likely delta oscillations are also involved. Whether that role is as an inhibitory mechanism or not remains unknown. Overall, when considering the time and frequency at which reliable differences were observed between accurate and guess trials, it seems likely that this post-target

activity reflects differences in the level of perceptual encoding of the target orientation and the subsequent precision of responses on the task.

Single-Trial EEG Activity and Response Errors

We were surprised to find no significant correlation between response error and oscillatory power in any of the measured frequencies, but this could also be attributed to the lack of sensitivity of the analysis method. Since failed to find support for our hypothesis regarding alpha oscillations, we chose to take a conservative approach when analyzing the rest of the time-frequency space. Using a less conservative method might help answer the question but that would increase the risk of finding false positives which could be more harmful than accepting false negatives.

Interestingly, we did find a relationship between response error and phase values in the delta and theta frequencies similar to the significant differences in mean phase of accurate trials compared to guess trials. In fact, phase modulation by response errors is even more pronounced than the differences in phase between accurate and guess trials. This strongly suggests delta and theta phase plays an important role in the amount of participants' response error on a trial-by-trial bases. Delta and theta frequencies are usually associated with working memory and cognitive control, but these results imply that they have an important role in visual perceptual processes as well.

Relationship Between Oscillatory Power and Standard Mixed Model Parameters

There were no significant correlations between oscillatory power and the guess rate parameter though there was a negative trend between guess rate and oscillatory power at the theta and alpha frequencies. However, in the fitting of the standard mixed model, there is always a slight negative correlation between the guess rate parameter and the standard deviation

parameter (Suchow et al., 2013). Consequently, the trend in correlations between guess rate and oscillatory power might be an artifact of the relationship between the guess rate parameter and the standard deviation parameter rather than a true association between oscillatory power and guess rate. This suggests that there is truly no significant correlation between guess rate and oscillatory power and points towards perception not operating by an all-or-none principle. However, correlations between guess rate and oscillatory power were more transient and in slightly lower frequencies than the correlations between power and the standard deviation parameter. In other words, the correlation between oscillatory power and guess rate are not what one would expect if they were mediated by the parameters' relationship. A relationship between guess rate and oscillatory might be worth investigating further with a task that purposefully changes the probability of guessing by alternating the detectability of the target.

Interestingly, frontal electrodes showed significant positive correlations between with the standard deviation parameter and power in the 3 Hz range during the onset of the response screen for around 50 ms. Accumulation of evidence has led investigators to associate frontal delta oscillations with top-down control and response inhibition (De Vries et al., 2018; Harmony, 2013; Helfrich et al., 2017; Rawls et al., 2020). Considering the significant relationship between delta activity and the standard deviation parameter is at the onset of the response screen, delta is likely being engaged for response inhibition instead of cognitive control. The positive correlation would further support this interpretation since an increase in response inhibition on a task that does not benefit from it would, at best, have little impact and, at worst, impair responding and increase response variability.

The significant positive correlation between alpha/low beta power and the standard deviation parameter provides further support for the idea that neural activity modulates the

quality of the perceptual representation rather than just its detection. The standard deviation parameter comes from the part of the standard mixed model representing trials where targets were seen and is meant to reflect the precision with which a participant perceived the target's orientation. It can be argued that the parameter also reflects the precision with which a participant gave responses (*i.e*., how carefully the participant oriented towards the response stimulus). However, the location of these significant correlations over non-motor areas (right medial parietal, parietooccipital and occipital electrodes) points toward the quality of perception being more of an influence on the standard deviation parameter than the motor-related precision with which participants responded.

If not motor-related, the question then is how decreases in high alpha/low beta power improved the quality of the perceptual representation? It has been demonstrated that decreases in alpha/low beta power correspond to an increase in cortical excitability (de Munck et al., 2007; Gonçalves et al., 2006; Iemi & Busch, 2018) and an increase in stimulus-specific information (Griffiths et al., 2019). Thus, our results could be interpreted as less alpha/low beta power mark enhanced processing of the target resulting in more precise perceptual representations of the target's orientation. At first these results might seem to go against the findings of the study by Bae and Luck (2018). However, another way to interpret their results could be that post-target alpha activity is more related to the encoding of the target's presence rather than specific features such as how the target was oriented. In that case, our results would be corroborating their findings and would explain why alpha/low beta tracks spatial location so well in attentional and working memory studies, but not the actual features of stimuli (Bae & Luck, 2019, 2018; Foster & Awh, 2019; Griffiths et al., 2019; Palomäki et al., 2012; Pesonen et al., 2007).

Conclusion

Overall, we have shown that the standard mixed model can be extended to a visual perception task and that doing so provides important insight into how brain activity shapes visual perception. Within-group results suggest that the difference between accurate responses and guesses are in the amount of post-target oscillatory activity in the delta and theta frequencies where greater activity was associated with smaller errors. This is evident by the significant differences between accurate and guess trials in power and phase at the delta and theta frequencies as well as the associated ERPs.

At the between-group level, those with lower post-target power in high alpha and low beta frequencies had more precision in their perceptual performance. This suggests that participants with greater cortical activity in the posterior regions have enhanced perceptual processing leading to a more precise perceptual representation of the targets' orientations. The posterior location of this activity precludes this being a motor-related effect.

Taken together, our results point towards a perceptual representation always forming but the quality, and thus, detectability, depends on the level of neural activity after stimulus onset. This is consistent with previous findings indicating that the brain holds stimulus information even when the stimulus is not consciously accessible to the participant and the difference between conscious and unconscious processing has to do with the difference in strength of the stimulus representation (Doradzińska et al., 2020; Mai et al., 2019).

It is important to note that our results are not suggesting pre-target EEG activity has no effect on visual perception. There is a lot of evidence to contrary. It is possible the analysis methods were not sensitive enough to pick up the trial-by-trial changes in pre-target activity, but it more likely there was no task-related modulation of pre-target activity due to participants

having no information about an upcoming trial. A follow-up study that directly manipulates attention or detectability of the target might be able to better test how differences in brain activity prior to target onset affect visual perception and subsequent task performance.

References

Auton, A. (2009). *Red Blue Colormap*. MATLAB Central File Exchange. https://www.mathworks.com/matlabcentral/fileexchange/25536-red-blue-colormap

Bae, G.-Y., & Luck, S. (2019). Appropriate Correction for Multiple Comparisons in Decoding of ERP Data: A Re-Analysis of Bae & Luck (2018). *BioRxiv*, Article 672741. https://doi.org/10.1101/672741

Bae, G.-Y., & Luck, S. J. (2018). Dissociable decoding of spatial attention and working memory from EEG oscillations and sustained potentials. *Journal of Neuroscience*, *38*(2), 409–422. https://doi.org/10.1523/JNEUROSCI.2860-17.2017

Barne, L. C., de Lange, F. P., & Cravo, A. M. (2020). Prestimulus alpha power is related to the strength of stimulus representation. *Cortex*, *132*, 250–257. https://doi.org/10.1016/j.cortex.2020.08.017

Başar, E., Başar-Eroglu, C., Karakaş, S., & Schürmann, M. (2001). Gamma, alpha, delta, and theta oscillations govern cognitive processes. *International Journal of Psychophysiology*, *39*(2–3), 241–248. https://doi.org/10.1016/S0167-8760(00)00145-8

Benjamini, Y., & Yekutieli, D. (2001). The control of the false discovery rate in multiple testing under dependency. *Annals of Statistics*, *29*(4), 1165–1188. https://doi.org/10.1214/aos/1013699998

Benwell, C. S. Y., Tagliabue, C. F., Veniero, D., Cecere, R., Savazzi, S., & Thut, G. (2017). Prestimulus EEG Power Predicts Conscious Awareness But Not Objective Visual Performance. *ENeuro*, *4*(6). https://doi.org/10.1523/ENEURO.0182-17.2017

Berens, P. (2009). CircStat: a MATLAB toolbox for circular statistics. *Journal of Statistical Software*, *31*(10), 679–685. https://doi.org/10.1016/j.amp.2012.05.023

Blair, R. C., & Karniski, W. (1993). An alternative method for significance testing of waveform difference potentials. *Psychophysiology*, *30*(5), 518–524. https://doi.org/10.1111/j.1469-8986.1993.tb02075.x

Brainard, D. H. (1997). The Psychophysics Toolbox. *Spatial Vision*, *10*(4), 433–436. http://www.ncbi.nlm.nih.gov/pubmed/9176952

Brüers, S., & VanRullen, R. (2017). At what latency does the phase of brain oscillations influence perception? *ENeuro*, *4*(3). https://doi.org/10.1523/ENEURO.0078-17.2017

Chaumon, M., & Busch, N. A. (2014). Prestimulus neural oscillations inhibit visual perception via modulation of response gain. *Journal of Cognitive Neuroscience*, *26*(11), 2514–2529. https://doi.org/10.1162/jocn_a_00653

Cohen, M. X. (2014). *Analyzing neural time series data: theory and practice*. MIT Press.

Cohen, M. X., & Cavanagh, J. F. (2011). Single-trial regression elucidates the role of prefrontal theta oscillations in response conflict. *Frontiers in Psychology*, *2*. https://doi.org/10.3389/fpsyg.2011.00030

Cohen, M. X., & Voytek, B. (2013). Linking nonlinear neural dynamics to single-trial human behavior. In M. (Meyer) Z. Pesenson (Ed.), *Multiscale Analysis and Nonlinear Dynamics* (pp. 217–232). Wiley-VCH Verlag GmbH & Co. KGaA. https://doi.org/10.1002/9783527671632

de Munck, J. C., Gonçalves, S. I., Huijboom, L., Kuijer, J. P. A., Pouwels, P. J. W., Heethaar, R. M., & Lopes da Silva, F. H. (2007). The hemodynamic response of the alpha rhythm: An EEG/fMRI study. *NeuroImage*, *35*(3), 1142–1151. https://doi.org/10.1016/j.neuroimage.2007.01.022

De Vries, I. E. J., Van Driel, J., Karacaoglu, M., & Olivers, C. N. L. (2018). Priority Switches in

Visual Working Memory are Supported by Frontal Delta and Posterior Alpha Interactions. *Cerebral Cortex*, *28*(11), 4090–4104. https://doi.org/10.1093/cercor/bhy223

Delorme, A., & Makeig, S. (2004). EEGLAB: An open source toolbox for analysis of single-trial EEG dynamics including independent component analysis. *Journal of Neuroscience Methods*, *134*(1), 9–21. https://doi.org/10.1016/J.JNEUMETH.2003.10.009

Di Russo, F., Berchicci, M., Bianco, V., Perri, R. L., Pitzalis, S., Quinzi, F., & Spinelli, D. (2019). Normative event-related potentials from sensory and cognitive tasks reveal occipital and frontal activities prior and following visual events. *NeuroImage*, *196*, 173–187. https://doi.org/10.1016/j.neuroimage.2019.04.033

Doradzińska, Ł., Wójcik, M. J., Paź, M., Nowicka, M. M., Nowicka, A., & Bola, M. (2020). Unconscious perception of one's own name modulates amplitude of the P3B ERP component. *Neuropsychologia*, *147*, 107564. https://doi.org/10.1016/j.neuropsychologia.2020.107564

Förster, J., Koivisto, M., & Revonsuo, A. (2020). ERP and MEG correlates of visual consciousness: The second decade. *Consciousness and Cognition*, *80*, Article 102917. https://doi.org/10.1016/j.concog.2020.102917

Foster, J. J., & Awh, E. (2019). The role of alpha oscillations in spatial attention: limited evidence for a suppression account. *Current Opinion in Psychology*, *29*, 34–40. https://doi.org/10.1016/J.COPSYC.2018.11.001

García-Pérez, M. A. (1998). Forced-choice staircases with fixed step sizes: asymptotic and small-sample properties. *Vision Research*, *38*(12), 1861–1881. https://doi.org/10.1016/S0042-6989(97)00340-4

Gonçalves, S. I., de Munck, J. C., Pouwels, P. J. W., Schoonhoven, R., Kuijer, J. P. A., Maurits, N.

M., Hoogduin, J. M., Van Someren, E. J. W., Heethaar, R. M., & Lopes da Silva, F. H. (2006). Correlating the alpha rhythm to BOLD using simultaneous EEG/fMRI: Inter-subject variability. *NeuroImage*, *30*(1), 203–213. https://doi.org/10.1016/j.neuroimage.2005.09.062

Grandchamp, R., & Delorme, A. (2011). Single-trial normalization for event-related spectral decomposition reduces sensitivity to noisy trials. *Frontiers in Psychology*, *2*, 236. https://doi.org/10.3389/fpsyg.2011.00236

Gratton, G., Coles, M. G. ., & Donchin, E. (1983). A new method for off-line removal of ocular artifact. *Electroencephalography and Clinical Neurophysiology*, *55*(4), 468–484. https://doi.org/10.1016/0013-4694(83)90135-9

Griffiths, B. J., Mayhew, S. D., Mullinger, K. J., Jorge, J., Charest, I., Wimber, M., & Hanslmayr, S. (2019). Alpha/beta power decreases track the fidelity of stimulus specific information. *ELife*, *8*, Article e49562. https://doi.org/10.7554/eLife.49562

Groppe, D. M., Urbach, T. P., & Kutas, M. (2011). Mass univariate analysis of event-related brain potentials/fields I: A critical tutorial review. *Psychophysiology*, *48*(12), 1711–1725. https://doi.org/10.1111/j.1469-8986.2011.01273.x

Harel, A., Groen, I. I. A., Kravitz, D. J., Deouell, L. Y., & Baker, C. I. (2016). The temporal dynamics of scene processing: A multifaceted EEG investigation. *ENeuro*, *3*(5), Article e0139-16.2016. https://doi.org/10.1523/ENEURO.0139-16.2016

Harmony, T. (2013). The functional significance of delta oscillations in cognitive processing. *Frontiers in Integrative Neuroscience*, *7*, Article 83. https://doi.org/10.3389/fnint.2013.00083

Harper, J., Malone, S. M., & Bernat, E. M. (2014). Theta and delta band activity explain N2 and P3 ERP component activity in a go/no-go task. *Clinical Neurophysiology*, *125*(1), 124–132.

https://doi.org/10.1016/j.clinph.2013.06.025

Helfrich, R. F., Huang, M., Wilson, G., & Knight, R. T. (2017). Prefrontal cortex modulates posterior alpha oscillations during top-down guided visual perception. *Proceedings of the National Academy of Sciences of the United States of America*, *114*(35), 9457–9462. https://doi.org/10.1073/pnas.1705965114

Helfrich, R. F., & Knight, R. T. (2019). Cognitive neurophysiology: Event-related potentials. In *Handbook of Clinical Neurology* (Vol. 160, pp. 543–558). Elsevier B.V. https://doi.org/10.1016/B978-0-444-64032-1.00036-9

Iemi, L., & Busch, N. A. (2018). Moment-to-moment fluctuations in neuronal excitability bias subjective perception rather than strategic decision-making. *ENeuro*, *5*(3), ENEURO.0430-17.2018. https://doi.org/10.1523/ENEURO.0430-17.2018

Iemi, L., Busch, N. A., Laudini, A., Haegens, S., Samaha, J., Villringer, A., & Nikulin, V. V. (2019). Multiple mechanisms link prestimulus neural oscillations to sensory responses. *ELife*, *8*, Article e43620. https://doi.org/10.7554/eLife.43620.001

Iemi, L., Chaumon, M., Crouzet, S. M., & Busch, N. A. (2017). Spontaneous neural oscillations bias perception by modulating baseline excitability. *Journal of Neuroscience*, *37*(4), 807–819. https://doi.org/10.1523/JNEUROSCI.1432-16.2016

Karakaş, S. (2020). A review of theta oscillation and its functional correlates. *International Journal of Psychophysiology*. https://doi.org/10.1016/j.ijpsycho.2020.04.008

Karakaş, S., Erzengin, Ö. U., & Başar, E. (2000). A new strategy involving multiple cognitive paradigms demonstrates that ERP components are determined by the superposition of oscillatory responses. *Clinical Neurophysiology*, *111*(10), 1719–1732. https://doi.org/10.1016/S1388-2457(00)00418-1

Keitel, C., Benwell, C. S. Y., Thut, G., & Gross, J. (2018). No changes in parieto-occipital alpha during neural phase locking to visual quasi-periodic theta-, alpha-, and beta-band stimulation. *European Journal of Neuroscience*, 1–15. https://doi.org/10.1111/ejn.13935

Key, A. P. F., Dove, G. O., & Maguire, M. J. (2005). Linking brainwaves to the brain: An ERP primer. *Developmental Neuropsychology*, *27*(2), 183–215. https://doi.org/10.1207/s15326942dn2702_1

Kingdom, F. A. A., & Prins, N. (2016). Chapter 5 – Adaptive Methods. In *Psychophysics* (Second Edi, pp. 119–148). Academic Press. https://doi.org/10.1016/B978-0-12-407156-8.00005-0

Klimesch, W. (1999). EEG alpha and theta oscillations reflect cognitive and memory performance: a review and analysis. *Brain Research Reviews*, *29*(2–3), 169–195. https://doi.org/10.1016/S0165-0173(98)00056-3

Koenig, L., & Ro, T. (2019). Dissociations of conscious and unconscious perception in TMS-induced blindsight. *Neuropsychologia*, *128*, 215–222. https://doi.org/10.1016/j.neuropsychologia.2018.03.028

Koivisto, M., & Revonsuo, A. (2003). An ERP study of change detection, change blindness, and visual awareness. *Psychophysiology*, *40*(3), 423–429. https://doi.org/10.1111/1469-8986.00044

Koivisto, M., & Revonsuo, A. (2010). Event-related brain potential correlates of visual awareness. *Neuroscience & Biobehavioral Reviews*, *34*(6), 922–934. https://doi.org/10.1016/j.neubiorev.2009.12.002

Limbach, K., & Corballis, P. M. (2016). Prestimulus alpha power influences response criterion in a detection task. *Psychophysiology*, *53*(8), 1154–1164. https://doi.org/10.1111/psyp.12666

Mai, A. T., Grootswagers, T., & Carlson, T. A. (2019). In search of consciousness: Examining the temporal dynamics of conscious visual perception using MEG time-series data. *Neuropsychologia*, *129*, 310–317. https://doi.org/10.1016/j.neuropsychologia.2019.04.015

Mathewson, K. E., Lleras, A., Beck, D. M., Fabiani, M., Ro, T., & Gratton, G. (2011). Pulsed out of awareness: EEG alpha oscillations represent a pulsed-inhibition of ongoing cortical processing. *Frontiers in Psychology*, *2*, Article 99. https://doi.org/10.3389/fpsyg.2011.00099

Palomäki, J., Kivikangas, M., Alafuzoff, A., Hakala, T., & Krause, C. M. (2012). Brain oscillatory 4-35 Hz EEG responses during an n-back task with complex visual stimuli. *Neuroscience Letters*, *516*(1), 141–145. https://doi.org/10.1016/j.neulet.2012.03.076

Pelli, D. G. (1997). The VideoToolbox software for visual psychophysics: transforming numbers into movies. *Spatial Vision*, *10*(4), 437–442. http://www.ncbi.nlm.nih.gov/pubmed/9176953

Pesonen, M., Hämäläinen, H., & Krause, C. M. (2007). Brain oscillatory 4–30 Hz responses during a visual n-back memory task with varying memory load. *Brain Research*, *1138*, 171–177. https://doi.org/10.1016/J.BRAINRES.2006.12.076

Potts, G. F., & Tucker, D. M. (2001). Frontal evaluation and posterior representation in target detection. *Cognitive Brain Research*, *11*(1), 147–156. https://doi.org/10.1016/S0926-6410(00)00075-6

Rawls, E., Miskovic, V., & Lamm, C. (2020). Delta phase reset predicts conflict-related changes in P3 amplitude and behavior. *Brain Research*, *1730*, 146662. https://doi.org/10.1016/j.brainres.2020.146662

Salti, M., Bar-Haim, Y., & Lamy, D. (2012). The P3 component of the ERP reflects conscious perception, not confidence. *Consciousness and Cognition*, *21*(2), 961–968. https://doi.org/10.1016/j.concog.2012.01.012

Samaha, J., Iemi, L., Haegens, S., & Busch, N. A. (2020). Spontaneous Brain Oscillations and Perceptual Decision-Making. *Trends in Cognitive Sciences*, *24*(8), 639–653. https://doi.org/10.1016/j.tics.2020.05.004

Samaha, J., Iemi, L., & Postle, B. R. (2017). Prestimulus alpha-band power biases visual discrimination confidence, but not accuracy. *Consciousness and Cognition*, *54*, 47–55. https://doi.org/10.1016/J.CONCOG.2017.02.005

Sauseng, P., Klimesch, W., Doppelmayr, M., Hanslmayr, S., Schabus, M., & Gruber, W. R. (2004). Theta coupling in the human electroencephalogram during a working memory task. *Neuroscience Letters*, *354*(2), 123–126. https://doi.org/10.1016/j.neulet.2003.10.002

Schürmann, M., Başar-Eroglu, C., Kolev, V., & Başar, E. (1995). A new metric for analyzing single-trial event-related potentials (ERPs): application to human visual P300 delta response. *Neuroscience Letters*, *197*(3), 167–170. https://doi.org/10.1016/0304-3940(95)11912-G

Schürmann, M., Başar-Eroglu, C., Kolev, V., & Başar, E. (2001). Delta responses and cognitive processing: Single-trial evaluations of human visual P300. *International Journal of Psychophysiology*, *39*(2–3), 229–239. https://doi.org/10.1016/S0167-8760(00)00144-6

Stouffer, S. A., Suchman, E. A., Devinney, L. C., Star, S. A., & Williams Jr., R. M. (1949). Studies in social psychology in World War II: the American soldier. In *Adjustment During Army Life* (Vol. 1). Princeton University Press. https://psycnet.apa.org/record/1950-00790-000

Suchow, J. W., Brady, T. F., Fougnie, D., & Alvarez, G. A. (2013). Modeling visual working memory with the MemToolbox. *Journal of Vision*, *13*(10), 1–8. https://doi.org/10.1167/13.10.9

van Diepen, R. M., & Mazaheri, A. (2018). The Caveats of observing Inter-Trial Phase-

Coherence in Cognitive Neuroscience. *Scientific Reports*, *8*(1), 2990. https://doi.org/10.1038/s41598-018-20423-z

VanRullen, R. (2016). How to Evaluate Phase Differences between Trial Groups in Ongoing Electrophysiological Signals. *Frontiers in Neuroscience*, *10*, 426. https://doi.org/10.3389/fnins.2016.00426

Zhang, W., & Luck, S. J. (2008). Discrete fixed-resolution representations in visual working memory. *Nature*, *453*(7192), 233–235. https://doi.org/10.1038/nature06860

Tables

Table 1

List of goodness-of-fit measures comparing the standard mixed model to the standard mixed model with a bias parameter (μ) for each participant.

	Log Likelihood			Bayesian Information Criterion (BIC)		
	Standard Model	Model + Bias	Difference	Standard Model	Model + Bias	Difference
Participant 1	-1255.82	-1255.33	-0.49	2526.45	2532.88	-6.44
Participant 2	-1213.93	-1212.78	-1.15	2442.77	2447.92	-5.15
Participant 3	-1095.28	-1094.58	-0.70	2205.45	2211.50	-6.05
Participant 4	-1093.29	-1093.24	-0.05	2201.25	2208.50	-7.24
Participant 5	-1191.23	-1190.92	-0.31	2397.23	2404.01	-6.77
Participant 6	-1113.21	-1111.14	-2.07	2241.28	2244.57	-3.29
Participant 7	-965.54	-964.92	-0.62	1945.90	1952.06	-6.16
Participant 8	-1022.30	-1021.07	-1.23	2059.48	2064.47	-4.99
Participant 9	-1109.18	-1109.12	-0.06	2233.12	2240.39	-7.27
Participant 10	-1422.57	-1422.42	-0.15	2859.94	2867.05	-7.11
Participant 11	-1384.47	-1384.46	-0.00	2783.78	2791.20	-7.42
Participant 12	-1017.58	-1015.52	-2.06	2049.58	2052.67	-3.09
Participant 13	-1498.89	-1498.55	-0.34	3012.59	3019.32	-6.73
Participant 14	-1071.57	-1071.55	-0.02	2157.98	2165.36	-7.38
Participant 15	-1124.71	-1123.84	-0.87	2264.26	2269.94	-5.68
Participant 16	-985.46	-985.17	-0.29	1985.36	1991.99	-6.63
Participant 17	-1149.36	-1149.26	-0.11	2313.61	2320.84	-7.23
Participant 18	-1136.58	-1136.50	-0.09	2287.86	2295.02	-7.17
Participant 19	-1133.03	-1132.91	-0.12	2280.88	2288.04	-7.16
Participant 20	-1276.89	-1275.81	-1.08	2568.44	2573.61	-5.17
Participant 21	-1138.27	-1133.04	-5.23	2291.40	2288.37	3.03[a]
Participant 22	-1003.69	-988.80	-14.89	2022.10	1999.69	22.41[a]
Participant 23	-1011.18	-1010.68	-0.50	2037.17	2043.57	-6.40
Participant 24	-1166.38	-1162.88	-3.49	2347.60	2348.04	-0.44

Note. Difference is calculated as the goodness-of-fit measure of the standard mixed model with a bias model subtracted from the goodness-of-fit measure of the standard mixed model.

[a] Positive difference indicates the standard mixed model with a bias parameter (μ) fits better to the participants' response errors (*i.e.*, has a smaller BIC) than the standard mixed model.

Figure Captions

Figure 1.

A) Sequence of task events with duration of each screen presentation and sizes of fixation, target, mask, and response stimuli. Sizes are in degrees of visual angle. **B)** Example of response error calculation. Response errors are reported in degrees.

Figure 2.

A) Representation of how trials were split into the two categories, Accurate and Guess. This was done by defining each participant's trials with response errors between -0.75σ and +0.75σ as "accurate" (shaded yellow region), and trials with response errors less than -1.5σ and greater than +1.5σ as "guesses" (shaded pink regions). Trials that did not fall in either category were discarded from this analyses between the two trial categories. **B)** Left, model fit of each participant. Right, solid purple line is the average of participants' model fit. Light purple area represents SEM. Zoomed in window shows upward shift of the averaged model fit showing a non-zero guess rate. **C)** Boxplots of parameter values (left) guess rate and (right) standard deviation estimated from model fits of participants' response errors.

Figure 3.

A) ERPs of accurate trials and guess trials aligned to target onset at selected electrodes and averaged across all electrodes (Grand Average). Light yellow and light pink shaded areas around waveforms represent ±SEM of accurate trials and guess trials, respectively. Mask trial EPRs have been subtracted out of the ERPs to remove mask-related brain activity except for the Grand Average + Mask ERPs plot. Time period shaded in green indicates significant difference between

accurate and guess trials 255-360 ms (N2) post-target. Blue shaded time period indicates significant difference between accurate and guess trials 360-500 ms (P3) post-target. **B)** Topographies of the voltage distribution difference between accurate and guess trials. The time periods in each topography are as follows: 200-255 ms (P2), 255-360 ms (N2), and 360-500 ms (P3) post-target. Stars indicate electrodes with significant differences between accurate and guess ERPs. Mask trial activity has been subtracted out of the ERPs to remove mask-related brain activity. **C)** Oscillatory power analysis of accurate vs guess trials. Time-frequency plots showing the results of the statistical analysis of the difference in power between accurate vs guess trials at each time-frequency point at selected electrodes and the average of all electrodes (Grand Average). Black contour denotes statistically significant differences (after applying the pixel-based multiple-comparison correction procedure) at $p < 0.05$. **D)** Oscillatory phase analysis of accurate vs guess trials. Time-frequency plots showing the *p*-values (after applying FDR correction) from the statistical analysis testing differences in the mean phase of accurate trials vs guess trials. Plots are from selected electrodes and the average of all electrodes (Grand Average). Time-frequency points with p-values above the threshold of FDR correction for multiple comparisons were set to 1.

Figure 4.

A) Example computation of weighted inter-trial phase clustering (wITPC) to relate single-trial phase to degree of response error. Top left, single-trial prestimulus phase vectors are shown as black lines and are not clustered across trials due to the randomization of the fixation length, leading to a low resultant vector length (i.e., low ITPC). Right, histogram of null-hypothesis vector lengths created by shuffling the mapping of the trial response error values to the trial

phase values. The observed vector length (large arrow) is calculated from the distribution shown in bottom left panel. Bottom left shows how the length each trial's phase vector is scaled by that trial's degree response error and a weighted ITPC is computed, reflecting the relationship between the distribution of phase angles and degree of response error even though the distribution of the phase angles themselves is uniform (as seen in the top left plot). The wITPCz value is the wITPC standardized relative to the null-hypothesis distribution seen in the histogram plot. Example based on figure by Cohen (2014) **B)** Time-frequency plots of analysis relating single-trial phase activity and response errors. Significant *p*-values indicating that the normalized distance of the observed wITPC (i.e., wITPCz) is significantly different from the distribution of null hypothesis wITPC values. This measure represents the relationship between the distribution of phase angles and the degree of response error on each trial. Plots are only of selected electrodes and the average of all electrodes (Grand Average). Time-frequency points with *p*-values at or above 0.05 were set to 1.

Figure 5.

Time-frequency plots showing the relationship between oscillatory power and the standard mixed model parameter standard deviation (σ) parameter. Standard deviation parameters were estimated by fitting the standard mixed model to each participants' set of response errors (Figure 2B and 2C). Dark gray contour denotes significant pixel-based corrected effects at $p < 0.05$. Scatterplots are bootstrap Spearman's rho (r_s) correlation coefficients of mean power across each statistically significant region outlined in black time. Arrows indicate which region on the time-frequency maps being plotted. Gray lines are bootstrapped least-squares correlation lines fit to 1000 bootstrap samples.

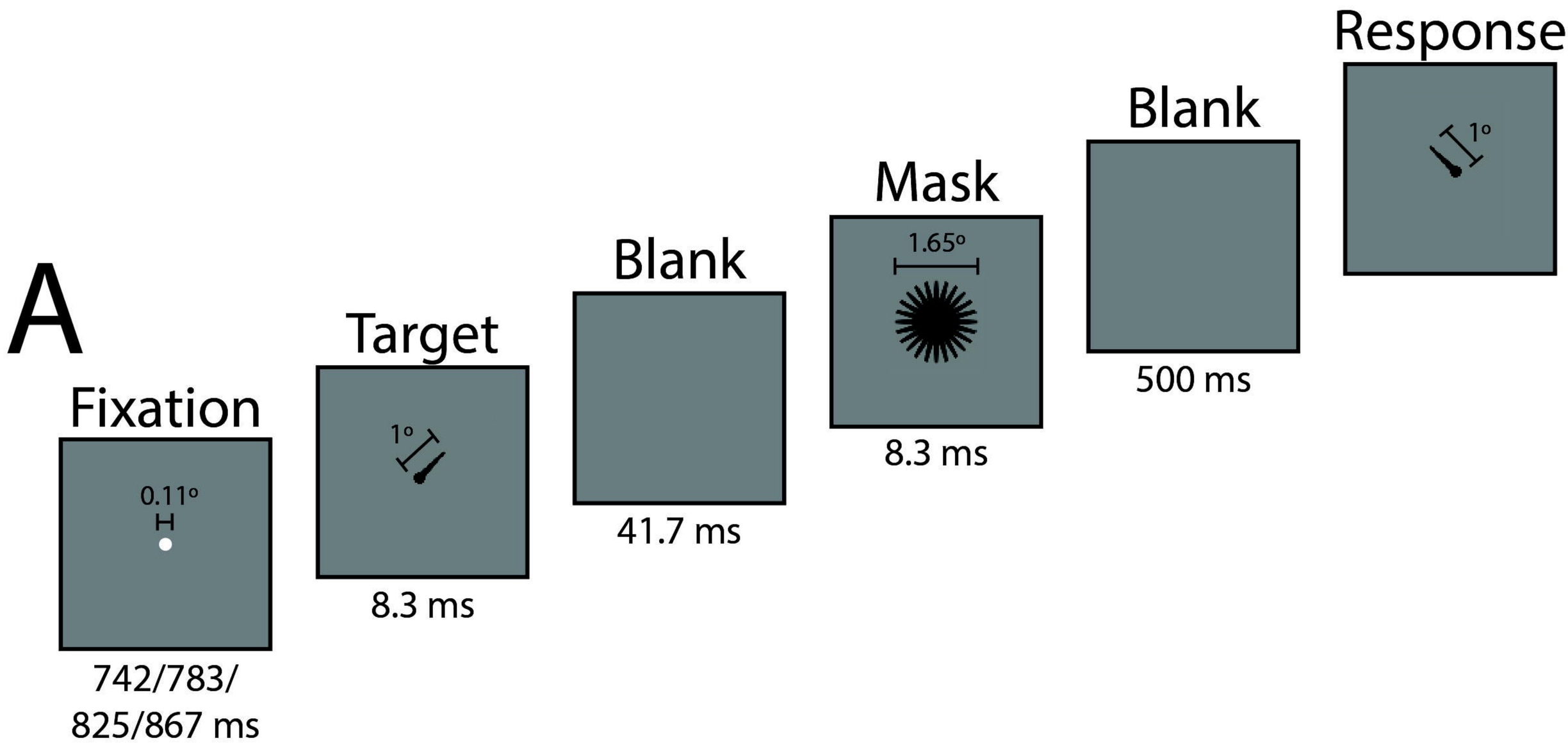
A
Fixation
0.11°
742/783/
825/867 ms
Target
1°
8.3 ms
Blank
41.7 ms
Mask
1.65°
8.3 ms
Blank
500 ms
Response
1°

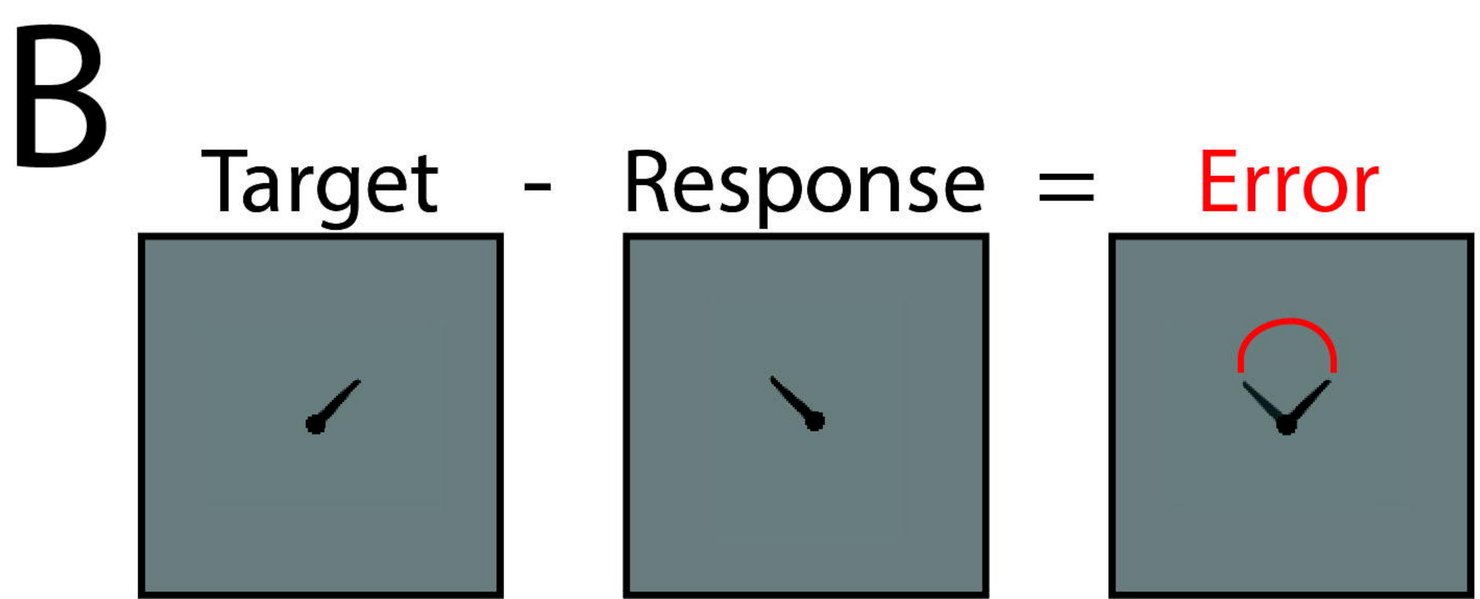
B
Target
-
Response
=
Error

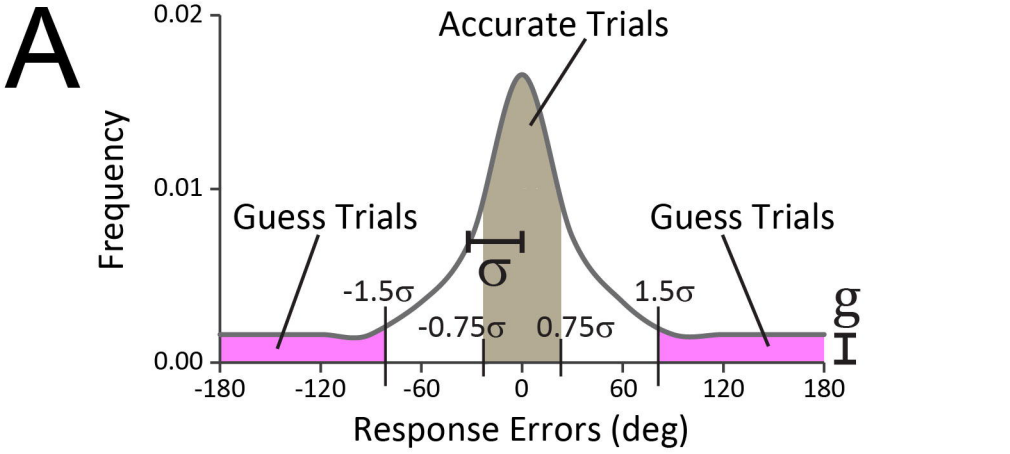
A
Accurate Trials
Frequency
0.02
0.01
0.00
Guess Trials
Guess Trials
σ
-1.5σ
1.5σ
-0.75σ
0.75σ
g
-180
-120
-60
0
60
120
180
Response Errors (deg)

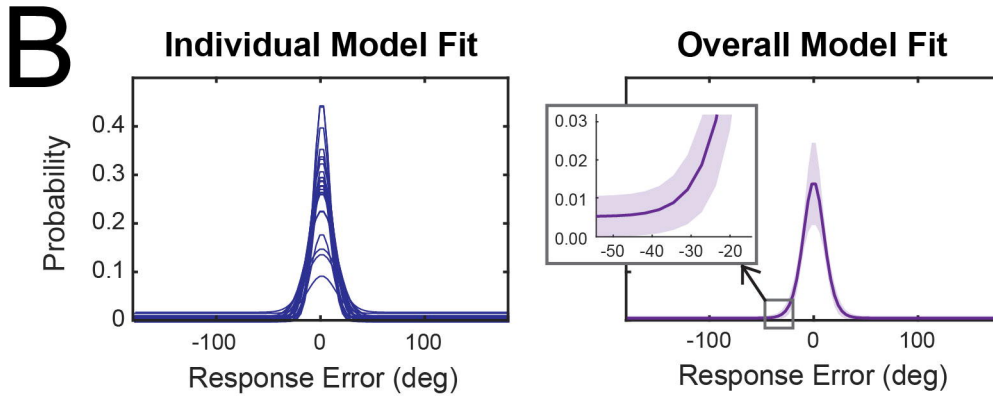
B
Individual Model Fit
Overall Model Fit
Probability
0.4
0.3
0.2
0.1
0
-100
0
100
Response Error (deg)
0.03
0.02
0.01
0.00
-50
-40
-30
-20
-100
0
100
Response Error (deg)

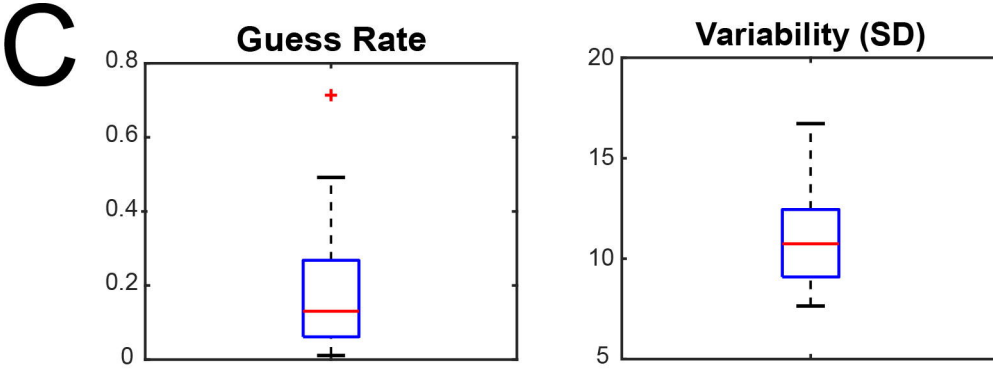
C
Guess Rate
0.8
0.6
0.4
0.2
0
Variability (SD)
20
15
10
5

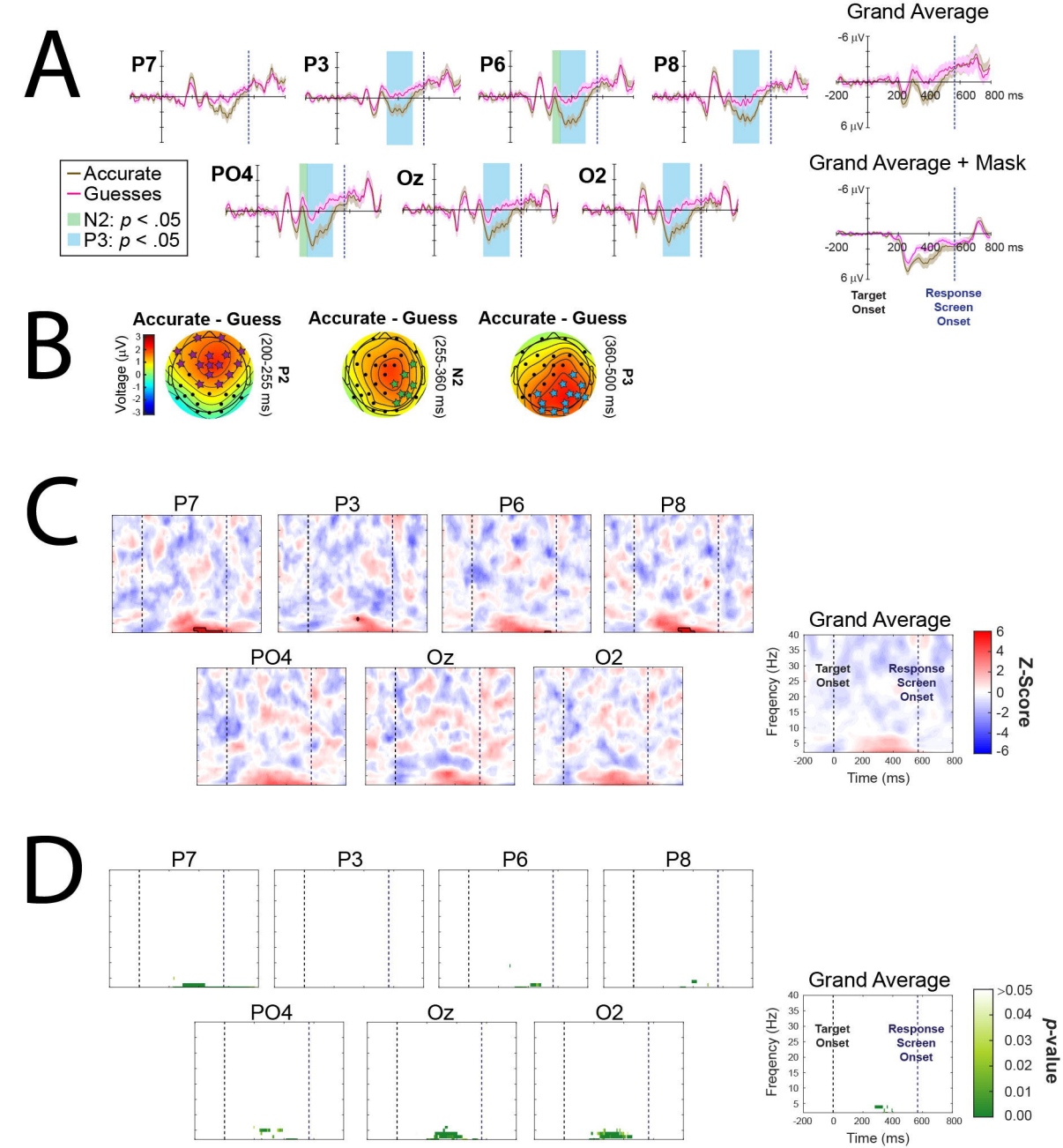
A
P7
P3
P6
P8
PO4
Oz
O2
Accurate
Guesses
N2: p < .05
P3: p < .05
Grand Average
-6 µV
6 µV
-200
200
400
600
800 ms
Grand Average + Mask
Target Onset
Response Screen Onset
B
Accurate - Guess
Voltage (µV)
P2 (200-255 ms)
N2 (255-360 ms)
P3 (360-500 ms)
C
Grand Average
Freqency (Hz)
Time (ms)
Z-Score
D
p-value
>0.05

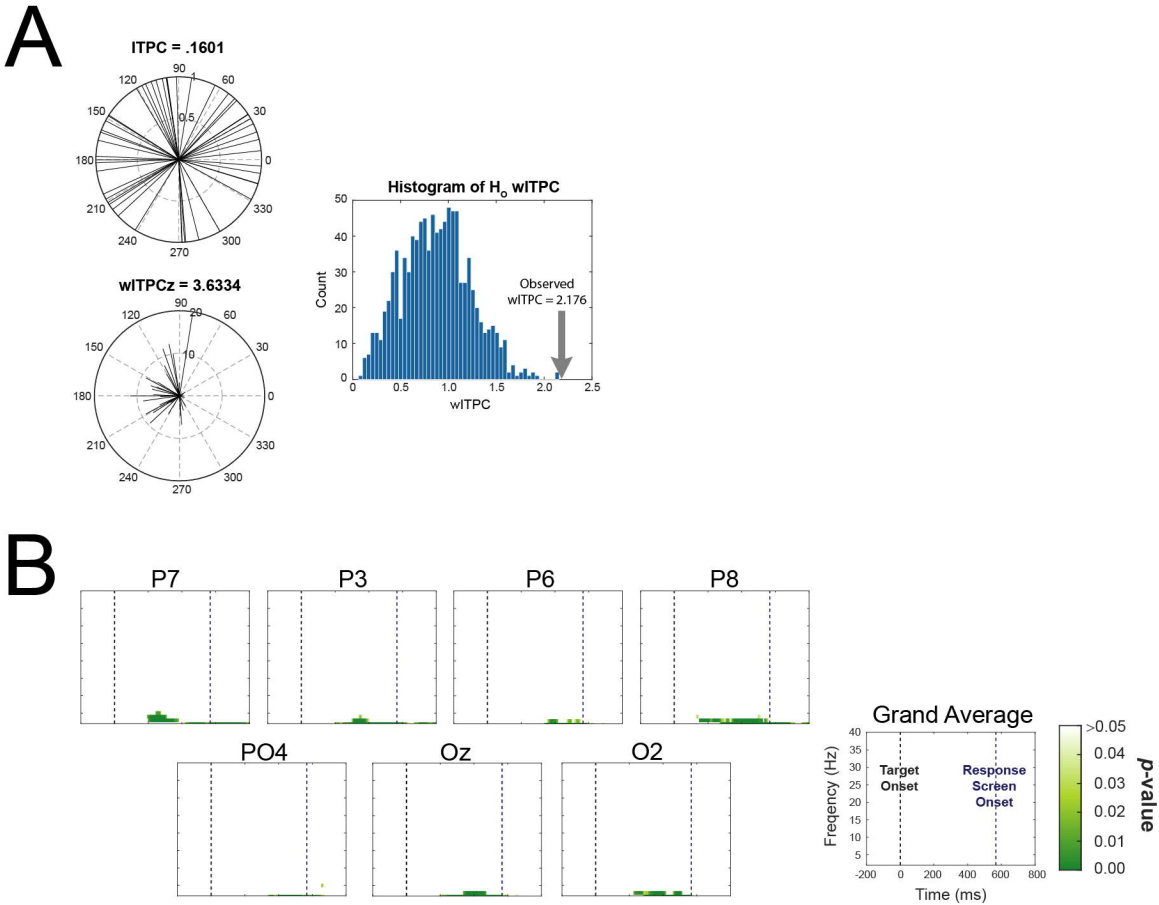
A
ITPC = .1601
wITPCz = 3.6334
Histogram of H$_o$ wITPC
Observed
wITPC = 2.176
Count
wITPC
B
P7
P3
P6
P8
PO4
Oz
O2
Grand Average
Target
Onset
Response
Screen
Onset
Freqency (Hz)
Time (ms)
p-value

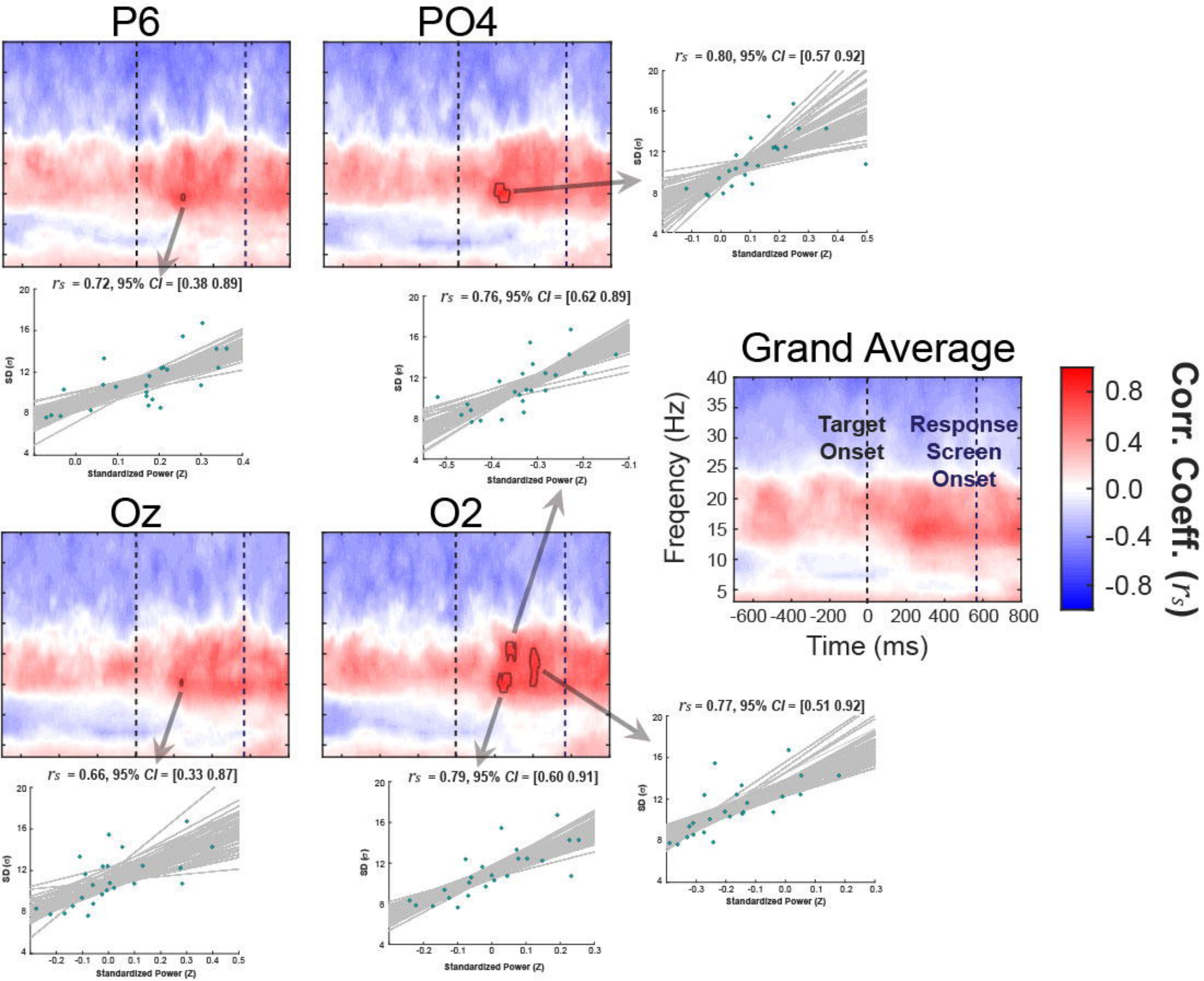
P6
PO4
rs = 0.80, 95% CI = [0.57 0.92]
rs = 0.72, 95% CI = [0.38 0.89]
rs = 0.76, 95% CI = [0.62 0.89]
Grand Average
Target Onset
Response Screen Onset
Freqency (Hz)
Time (ms)
Corr. Coeff. (rs)
Oz
O2
rs = 0.77, 95% CI = [0.51 0.92]
rs = 0.66, 95% CI = [0.33 0.87]
rs = 0.79, 95% CI = [0.60 0.91]
SD (σ)
Standardized Power (Z)